

Electronic Spectrum of Silicon Monosulfide: Configuration Interaction Study

Surya Chattopadhyaya, Anjan Chattopadhyay, and Kalyan Kumar Das*

Department of Chemistry, Physical Chemistry Section, Jadavpur University, Kolkata 700 032, India

Received: August 28, 2001; In Final Form: November 5, 2001

Ab initio based configuration interaction calculations using relativistic effective core potentials and compatible basis sets have been performed to study the electronic spectrum of the silicon monosulfide molecule. Potential energy curves of low-lying states of SiS have been computed. Spectroscopic properties of many observed states such as $X^1\Sigma^+$, $a^3\Sigma^+$, $d^3\Delta$, $b^3\Pi$, $C^1\Sigma^-$, $e^3\Sigma^-$, $D^1\Delta$, $A^1\Pi$, and $E^1\Sigma^+$ up to $42\,000\text{ cm}^{-1}$ of energy have been calculated and compared. The ground state of SiS is represented mainly by $\dots\pi^4$ (74%) and $\dots\pi^3\pi^*$ (12%) configurations with $r_e = 1.957\text{ \AA}$ ($3.7 a_0$) and $\omega_e = 733\text{ cm}^{-1}$, which compare well with the observed values. The dissociation energies of the ground and excited states have been estimated. All 18 Λ -S states correlating with the lowest asymptote have been allowed to mix through the spin-orbit coupling. Effects of spin-orbit interactions on the potential energy curves and spectroscopic properties of the low-lying states of SiS are studied. Dipole-allowed transitions such as E-X and A-X are found to be strong. Several spin-forbidden weak transitions are also noted. The radiative lifetimes of many upper states are estimated. The $E^1\Sigma_0^+$ and $A^1\Pi_1$ states are predicted to be short-lived with radiative lifetimes of about 10.2 and 103 ns, respectively.

I. Introduction

Over the past few decades,^{1–18} there has been a significant increase in the amount of experimental and theoretical data on the spectroscopy of diatomic molecules of group IV/VI atoms. The compounds of germanium and silicon are known to be good semiconducting materials. Barrow and co-workers^{1–8} have made pioneering research on these molecules. The red-degraded emission bands in the electric discharge through argon and the vapor of SiS have been observed by Barrow and Jevons.¹ It has been concluded that these bands in the 3500–6200 Å region appear from a transition between two electronic states of the SiS radical. However, the nature of these states could not be established at that time. Later on, Lagerqvist et al.⁷ have tentatively assigned the upper state involved in this transition as the $E^1\Sigma^+$ state of SiS. Two electronic transitions for the SiS molecule involving singlets, namely, $D^1\Pi-X^1\Sigma^+$ and $E^1\Sigma^+-X^1\Sigma^+$ are also observed by many authors.^{8,9} The D-X band system has been known in the near-ultraviolet region for each of SiX (X = S, Se, Te) molecules, and it appears readily in emission in positive-column discharges.^{3,4} The D-X system has been photographed in absorption as well. Vago and Barrow⁵ have observed a new ultraviolet E-X band system for SiS, SiSe, and SiTe molecules in absorption at the temperature range 800–1000 °C. The vibrational constants of X, D, and E states of these molecules are estimated from the spectra. The X and D states are assigned to $^1\Sigma^+$ and $^1\Pi$ symmetries, respectively. In a subsequent study,⁶ the rotational analysis of the $D^1\Pi-X^1\Sigma^+$ band of SiS in the near-ultraviolet region has been performed. Spectroscopic constants of $X^1\Sigma^+$ and $D^1\Pi$ states are estimated from the rotational analysis. The equilibrium bond lengths of the ground and $D^1\Pi$ states are reported to be 1.929 and 2.059 Å, respectively. The rotational analysis of twenty bands of the E-X system of SiS has been carried out by Barrow et al.¹⁰

The shorter-wavelength band with $\nu_{00} = 41\,744\text{ cm}^{-1}$ has been proved to be due to the $^1\Sigma^+-^1\Sigma^+$ transition. It has been suggested that the E state is an excited $^1\Sigma^+$ arising from the $\dots\pi^3\sigma^2\pi^*$ configuration analogous to the $B^1\Sigma_u^+$ state of P_2 . Meyer et al.¹¹ have measured the lifetimes of the spin-forbidden Cameron bands ($a^3\Pi-X^1\Sigma^+$) of GeO, GeS, SnO, and SnS in inert-gas matrices and SF₆. These authors have also predicted lifetimes of the same Cameron bands for CO, CS, SiO, and SiS. For the SiS molecule in argon at 20 K, the predicted lifetime of the $^3\Pi$ state is about 29 ms.

Bredohl et al.¹² have reobserved the $E^1\Sigma^+-X^1\Sigma^+$ transition for SiS with $\nu_{00} = 41\,915.7\text{ cm}^{-1}$ using high-resolution spectra. A spin-forbidden $a^3\Pi_r-X^1\Sigma^+$ transition of SiS is also observed in emission by Bredohl et al.¹³ This transition is analogous to those observed in the isovalent SiO and SiSe molecules. For SiS, a vibrational progression of five bands has been reported in this system. Linton¹⁴ has investigated the spectra of SiS molecules produced in the flame of the chemiluminescent reaction of atomic silicon with OCS. Two new band systems in the region 350–400 and 385–600 nm have been assigned as $b^3\Pi_r-X^1\Sigma^+$ and $a^3\Sigma^+-X^1\Sigma^+$, respectively based on band structure, spin-orbit splitting, molecular constants, and comparison with chemiluminescent spectra of isovalent molecules. The vibrational assignments of these bands are made with the help of isotope effect. The spin-orbit separations for the components of $^3\Pi$ at $v' = 0$ are found to be $^3\Pi_1-^3\Pi_0 = 96\text{ cm}^{-1}$ and $^3\Pi_2-^3\Pi_1 = 61\text{ cm}^{-1}$. These studies reveal that the $^3\Pi_1-^3\Pi_0$ separation increases rapidly with v' . The $^3\Pi_0$ component is found to be more intense than expected. The spin-orbit mixing between $A^1\Pi$ and $b^3\Pi$ states borrows the intensity to the $^3\Pi-^1\Sigma^+$ transition. Linton¹⁴ has observed irregularities in the relative intensities of the spin-orbit components and their splitting in the $b^3\Pi-X^1\Sigma^+$ system. These are explained by the interactions with the nearby states such as $E^1\Sigma^+$, $D^1\Delta$, and $d^3\Delta$. It has been found that after adding active nitrogen in the

* Author for correspondences. E-mail: kalyankd@hotmail.com; das_kalyank@yahoo.com.

chemiluminescent flame, the intensity of the $b-X$ transition is enhanced largely as compared with that of the $a-X$ transition.

A detailed rotational analysis of bands of the $A^1\Pi-X^1\Sigma^+$ system of ^{28}SiS and ^{30}SiS isotopes has been carried out by Harris et al.¹⁵ These studies reveal identification and determination of vibrational numbering of perturbing states such as $e^3\Sigma^-$, $d^3\Delta$, $C^1\Sigma^-$, and $D^1\Delta$. Two alternative consecutive vibrational numbers for $D^1\Delta$ are suggested. The electronic interaction constants are derived for the interactions between $A^1\Pi$ and the perturbing states. It may be mentioned that some of the excited states of SiS are relabeled to conform to the nomenclature used for SiO. Krishnamurty et al.¹⁶ have made similar rotational analysis of thirteen bands of the $A^1\Pi-X^1\Sigma^+$ system lying in the region 2600–3000 Å. The molecular constants of the $A^1\Pi$ state have been evaluated from the high-resolution studies. Perturbations in the bands of $A^1\Pi-X^1\Sigma^+$ have been attributed to the same four excited states as observed by Harris et al.¹⁵ The band origins involving $v' = 2, 6, \text{ and } 7$ have been found to be shifted from the expected positions due to such perturbations. The infrared spectra of many isovalent matrix-isolated germanium, tin, and lead chalcogenides have been carried out by Marino et al.¹⁷ Although many experimental studies are available for SiS, theoretical calculations are seldom attempted. Relativistic configuration interaction calculations of heavy molecules and clusters have been reviewed by Balasubramanian.^{18,19} Robbe et al.²⁰ have performed ab initio based configuration interaction (CI) calculations for the wave functions, energies, and spectroscopic parameters of low-lying electronic states of SiS. These authors have also calculated theoretical perturbation parameters involving the $A^1\Pi$ state. Recently,^{21–23} ab initio based CI calculations on the low-lying excited states of isovalent molecules such as GeS, GeSe, and GeTe have been performed. These studies have also revealed spectroscopic features and potential energy curves of excited states of these molecules.

The present paper deals with the computations of potential energy curves and electronic spectrum of low-lying states of SiS by employing multireference singles and doubles configuration interaction (MRDCI) method, which includes relativistic effective core potentials (RECP). Spin-orbit interactions, which allow the spin-forbidden transitions to occur, are studied extensively. The present calculations will take care of the estimation of transition probabilities of dipole-allowed and spin-forbidden transitions with a special reference to experimental findings. Radiative lifetimes of many low-lying excited states of SiS are also reported.

II. Details of the Computations

The RECP of both Si and S are taken from Pacios and Christiansen²⁴ to describe the inner electrons of the atoms. In other words, the $3s^23p^2$ electrons of Si and $3s^23p^4$ electrons of S have been kept in the valence space, whereas the remaining inner electrons are substituted with the effective potentials, which reduce the number of active electrons to 10. The (4s4p) primitive Gaussian basis sets²⁴ of Si are augmented with a set of d polarization functions²⁵ with an exponent of $0.30 a_0^{-2}$. A second set of semidiffuse d-type Gaussian functions²⁶ with an exponent of $0.05 a_0^{-2}$ is also added in the basis set of Si. An additional set of semidiffuse p functions^{27,28} ($\xi_p = 0.027 a_0^{-2}$) is included for the better description of 3p orbitals of Si. Thus, the final basis set for Si becomes (4s5p2d). For the sulfur atom, the basis set of Pacios and Christiansen²⁴ is extended by adding two-member d polarization functions of the exponents 0.66 and $0.18 a_0^{-2}$, which are optimized by Lingott et al.²⁹ for the 3P state of S at the CI level. A set of f functions with an exponent

of $0.90 a_0^{-2}$ optimized from the CI calculations of the 1D excited atomic state has been included in the basis set of the sulfur atom.²⁹ The resulting basis set of the sulfur atom in the present calculations is (4s4p2d1f), which is sufficient to describe 3s and 3p orbitals of the atom. The basis sets of both silicon and sulfur atoms are, therefore, compatible with their RECP.

Self-consistent field (SCF) calculations have been carried out for the $... \pi^4 \pi^{*2} {}^3\Sigma^-$ state of SiS at each internuclear distance by employing the basis sets and RECP mentioned above. The calculations generate 69 symmetry-adapted SCF-MOs, which are taken as one-electron basis functions for the CI calculations. Ten valence electrons are allowed to excite in the CI steps. The molecule has been kept along the z -axis. We have performed the entire computations in the C_{2v} subgroup of the actual $C_{\infty v}$ group in which the molecule belongs. The MRDCI codes of Buenker and co-workers^{30–35} are used throughout the calculations. The open-shell configurations are taken into consideration by the table-CI algorithm. In the first step, the Λ -S states are calculated including all relativistic effects but the spin-orbit coupling through RECP. A set of reference configurations has been chosen for the low-lying states of a given spatial and spin symmetry. In the present calculations, we have computed eight lowest roots for each Λ -S symmetry of singlet and triplet spin multiplicities, whereas for quintets only four roots are considered. These reference configurations describe the low-lying excited states throughout the potential energy curve. Single and double excitations are allowed from each of these reference configurations. As a result, a large number of configurations, up to six million, is generated for a given irreducible representation. However, the configuration-selection and extrapolation technique are used to reduce the size of the secular equation. The higher-order excitations with respect to the reference configurations are taken into consideration by using the Davidson correction³⁶ to the MRDCI-estimated extrapolated energies for each root. The configuration-selection threshold has been kept at $5 \mu\text{hartree}$ throughout the calculations so that the largest dimension of the selected CI space does not exceed 50 000. The sum of the squares of coefficients of the reference configurations for each root remains always above 0.90. The CI wave functions and estimated full-CI energies of the Λ -S states are used for the computation of spectroscopic constants and transition properties of the SiS molecule.

In the next step, the spin-orbit coupling is introduced into the calculations by employing the spin-orbit operators,²⁴ which are compatible with RECP of Si and S. After the spin-orbit interaction, the Ω states are classified into A_1 , A_2 , and B_1 representations of the C_{2v}^2 group. The B_2 irreducible representation is degenerate with B_1 , hence states belonging to B_2 are not computed. The Λ -S CI wave functions are taken as basis for the spin-orbit CI calculations. The estimated full-CI energies in the Λ -S calculations are placed in the diagonals of the Hamiltonian matrix, while the off-diagonal elements are calculated from the RECP-based spin-orbit operators and Λ -S CI wave functions. All 18 Λ -S states, which correlate with the $\text{Si}(^3P_g) + \text{S}(^3P_g)$ limit, are included in the spin-orbit CI treatment. The sizes of three secular blocks A_1 , A_2 , and B_1 are 51, 50, and 51, respectively. In the two-step procedure for the inclusion of the spin-orbit interaction, the resulting wave functions of Ω states can be easily analyzed in terms of different Λ -S eigenfunctions. Spectroscopic constants of both Λ -S as well as Ω states are estimated by fitting the potential energy curves of all bound low-lying states of SiS. Using the fitted potentials, nuclear Schrödinger equations are solved numerically to obtain vibrational energies and wave functions. Subsequently, transition

dipole moments for the pair of vibrational functions involved in a particular transition are computed. The spontaneous emission coefficients and transition probabilities are calculated in the following way.

The Einstein spontaneous emission coefficients $A_{v'v''}$ (in s^{-1}) between vibrational levels (v') of the upper state and vibrational levels (v'') of the lower electronic state are written as

$$A_{v'v''} = g_{e'e''} [2.1419 \times 10^{10} (\Delta E)^3 S_{v'v''}]$$

where

$$S_{v'v''} = |\langle \chi_{v''}(r) \mathbf{R}_{e'e''}(r) \chi_{v'}(r) \rangle|^2$$

and ΔE is the transition energy value in a.u. $S_{v'v''}$ is obtained from a polynomial fit to the set of data for the electronic transition moment $\mathbf{R}_{e'e''}$ and vibrational wave functions $\chi_v(r)$ generated for the respective pairs of electronic states.^{37–39} The term $g_{e'e''}$ is the degeneracy factor. The radiative lifetime of a given vibrational level (v') of the upper electronic state is obtained from $(1/\sum_{v''} A_{v'v''})$.

III. Potential Energy Curves and Spectroscopic Constants of Λ -S States

Parts a–c of Figure 1 show the computed potential energy curves of the low-lying singlet, triplet, and quintet Λ -S states of the SiS molecule from the MRDCI treatment using the spin-independent Hamiltonian. The lowest dissociation limit $\text{Si}(3p^2, ^3P_g) + \text{S}(3p^4, ^3P_g)$ of SiS correlates with eighteen Λ -S states of singlet, triplet, and quintet spin multiplicities. The interaction of the excited $\text{Si}(3p^2, ^1D_g)$ atom with the ground-state S atom generates only nine triplet states. The experimental relative energy (averaged over j) of the 1D_g state of Si is about 6125 cm^{-1} as compared with the value of 8081 cm^{-1} calculated at the Λ -S level. The dissociation correlations between the atomic and Λ -S states of SiS are shown in Table 1. In the present computations, we are mainly concerned with those Λ -S states that correlate with the lowest dissociation limit of the molecule. However, some other high-lying states are also reported. Spectroscopic constants (r_e , ω_e , and T_e) of several Λ -S states up to 8 eV are given in Table 2. The ground state ($X^1\Sigma^+$) of SiS has the shortest equilibrium bond length [$r_e = 1.957 \text{ \AA}$ ($3.7 a_0$)] of all Λ -S states computed here. The calculated ground-state bond length is larger than the value estimated from the rotational analysis of the $D^1\Pi - X^1\Sigma^+$ band system by about 0.028 \AA . A discrepancy of a similar magnitude has been noted for the ground state of the isovalent GeS molecule calculated at the same level.²¹ The vibrational frequency of the ground state at r_e is calculated to be 733 cm^{-1} , which agrees well with the observed value of 749.64 cm^{-1} . Earlier calculations using the same MRDCI method suggest that the discrepancy is within the accuracy of the CI treatment under the effective core potential approximation. The limited SCF–CI calculations of Robbe et al.²⁰ have estimated the ω_e value of 795 cm^{-1} for the ground state of SiS. The ground state at r_e is not represented by a single configuration. The dominant closed-shell configuration $\dots\sigma^2\sigma^*\sigma^2\pi^4$ ($c^2 = 0.74$) is mixed with a singly excited ($\pi \rightarrow \pi^*$) configuration such as $\dots\sigma^2\sigma^*\sigma^2\pi^3\pi^*$ having $c^2 = 0.12$. Analyzing the SCF-MOs at the ground-state geometry of the molecule, it is found that σ and σ^* are strongly bonding and antibonding MOs, comprising s , $p_z(\text{Si})$ and s , $p_z(\text{S})$ atomic orbitals, respectively. Third σ -orbital, which is denoted here as σ' , is bonding with respect to p_z orbitals of Si and S atoms, while π and π^* MOs are, respectively bonding and antibonding

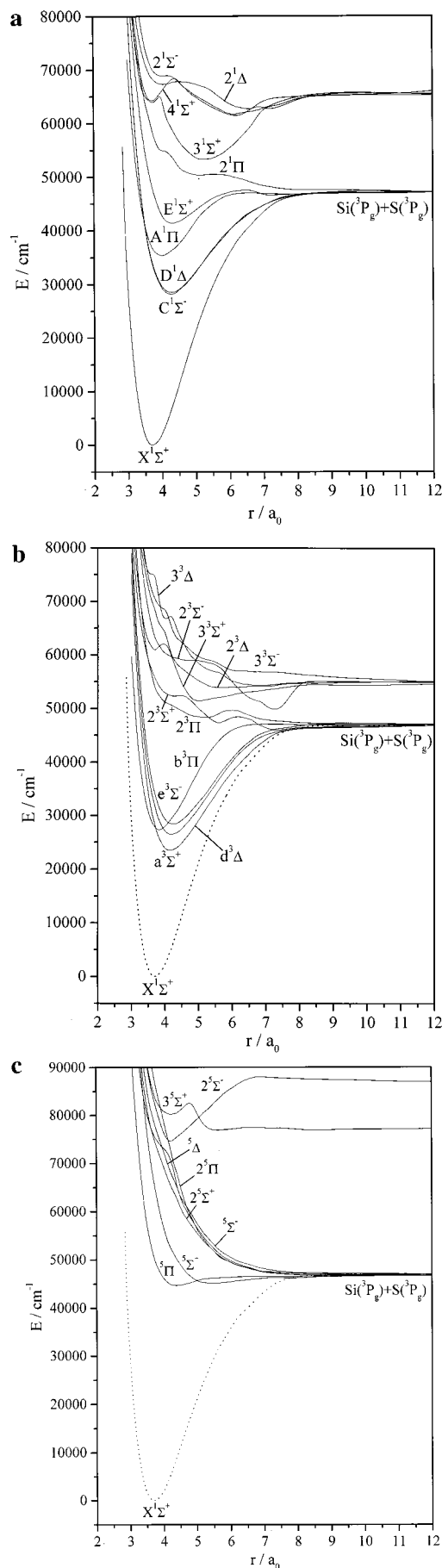


Figure 1. (a) Potential energy curves of low-lying singlet Λ -S states of SiS. (b) Potential energy curves of low-lying triplet Λ -S states of SiS. (c) Potential energy curves of low-lying quintet Λ -S states of SiS.

TABLE 1: Correlation between the Atomic and Λ -S States of SiS

Λ -S states	atomic states (Si + S)	relative energy/cm ⁻¹	
		expt ^a	calc
¹ $\Sigma^+(2)$, ¹ Σ^- , ¹ $\Pi(2)$, ¹ Δ ,	(3p ²) ³ P _g + (3p ⁴) ³ P _g	0	0
³ $\Sigma^+(2)$, ³ Σ^- , ³ $\Pi(2)$, ³ Δ ,			
⁵ $\Sigma^+(2)$, ⁵ Σ^- , ⁵ $\Pi(2)$, ⁵ Δ			
³ Σ^+ , ³ $\Sigma^-(2)$, ³ $\Pi(3)$, ³ $\Delta(2)$,	(3p ²) ¹ D _g + (3p ⁴) ³ P _g	6125	8081
³ Φ			

^a Reference 41.**TABLE 2: Spectroscopic Constants of the Λ -S States of SiS**

state	T_e /cm ⁻¹		r_e /Å		ω_e /cm ⁻¹	
	calc	expt	calc	expt	calc	expt
X ¹ Σ^+	0	0	1.957	1.929 ^a	733	749.64 ^{a,b}
a ³ Σ^+	23 518	24 582 ^d	2.195		504	503.8 ^d
	(24 160) ^c				(580) ^c	
d ³ Δ	26 502	27 233 ^e	2.220	2.169 ^{e,f}	480	487.3 ^e
	(27 460) ^c	27 268 ^g			(525) ^c	477.82 ^g
b ³ Π	27 378	27 314.5 ^{d,h}	2.026		604	619.4 ^h
	(29 100) ^c	27 407.9 ^{d,i}			(530) ^c	624.3 ⁱ
C ¹ Σ^-	28 235	29 072 ^e	2.254	2.197 ^e	467	463 ^e
	(29 360) ^c	28 972.8 ^g			(480) ^c	465.8 ^g
e ³ Σ^-	28 420	29 162 ^e	2.242	2.192 ^e	462	464.4 ^e
	(29 540) ^c	29 112 ^g			(490) ^c	463.03 ^g
D ¹ Δ	28 532	28 919 ^e	2.262	2.191 ^e	445	470.1 ^e
	(29 740) ^c	28 906 ^g			(470) ^c	462.47 ^g
A ¹ Π	35 385	35 026.84 ^e	2.112	2.059 ^a	485	513.17 ^e
	(38 070) ^c	35 026.69 ^g			(510) ^c	506.04 ^g
E ¹ Σ^+	41 383	41 915.8 ^b	2.286	2.259 ^e	418	405.6 ^b
	(48 000) ^c				(330) ^c	
⁵ Π	44 870		2.342		283	
⁵ Σ^+	45 225		2.904		168	
³ ¹ Σ^+	53 328		2.805		282	
⁴ ¹ Σ^+	64 288		1.973		686	

^a Reference 6. ^b Reference 12. ^c Reference 18. ^d Reference 14. ^e Reference 15. ^f Value is for the component d³ Δ_1 . ^g Reference 16. ^h Value is for the ³ Π_0 component. ⁱ Value is for the ³ Π_1 component.

combinations of $p_{x(y)}$ (Si) and $p_{x(y)}$ (S) atomic orbitals. In π MO, the contribution of $p_{x(y)}$ (S) is large, while the atomic orbital $p_{x(y)}$ (Si) dominates in the π^* MO. The computed transition energy of the first excited state (a³ Σ^+) is 23 518 cm⁻¹, which is underestimated by about 1000 cm⁻¹. After examining the spectra of the chemiluminescent flame consisting of the a³ Σ^+ –X¹ Σ^+ band system, Linton¹⁴ has observed the a³ Σ^+ state at 24 582.1 ± 1.3 with $\omega_e = 503.8 \pm 1.0$ cm⁻¹. The calculated ω_e of the a³ Σ^+ state matches almost exactly with the observed value. On the other hand, the small-scale SCF–CI calculations of Robbe et al.²⁰ show a better agreement of T_e of the a³ Σ^+ state, while its vibrational frequency is overestimated by about 76 cm⁻¹. The a³ Σ^+ state of SiS is analogous to a³ Σ^+ of the isovalent CO molecule. There seems to be no experimental data for r_e of the a³ Σ^+ state to verify the MRDCI-estimated value of 2.195 Å (4.15 a_0). However, we expect the observed r_e would be lower than the calculated value by 0.03–0.05 Å. The binding energy of the molecule in the a³ Σ^+ state obtained from the MRDCI treatment is found to be 2.94 eV. The Si–S bond in the a³ Σ^+ state is found to be weaker than the ground-state bond. The compositions of CI wave functions show that the a³ Σ^+ state is predominantly characterized by a singly excited ($\pi \rightarrow \pi^*$) configuration.

Besides a³ Σ^+ , five other Λ -S states such as ³ Σ^- , ³ Δ , ¹ Σ^+ , ¹ Σ^- , and ¹ Δ are generated due to the $\pi \rightarrow \pi^*$ excitation. All six states dissociate into the lowest asymptote Si(³P_g) + S(³P_g). As seen from Table 2, the lowest state of the ³ Δ symmetry,

which is denoted as d³ Δ , is lying 26 502 cm⁻¹ above the ground state. The spectroscopic studies of Harris et al.¹⁵ and Krishnamurthy et al.¹⁶ suggest that the transition energy of d³ Δ is in the range 27 233–27 268 cm⁻¹. The T_e value computed here is also smaller than the small-scale CI result of Robbe et al.²⁰ On the other hand, the MRDCI-estimated ω_e value of the d³ Δ state is in excellent agreement with the observed value, whereas the small-scale CI of Robbe et al.²⁰ has reported a somewhat larger ω_e value. The computed r_e of the d³ Δ state is 2.22 Å (4.2 a_0) as compared with the observed value¹⁵ of 2.169 Å for the d³ Δ_1 component. The discrepancies in r_e values are more or less consistent throughout the calculations. The next triplet state of the ³ Σ^- symmetry is designated as e³ Σ^- , which has the same dominating $... \sigma^2 \sigma^{*2} \sigma'^2 \pi^3 \pi^*$ ($c^2 = 0.86$) configuration as those in a³ Σ^+ and ³ Δ states. Potential energy curve and molecular constants of the e³ Σ^- state are also known experimentally.¹⁵ In Figure 1b, we have plotted the calculated potential energies of the e³ Σ^- state along with other low-lying triplets of SiS. The computed transition energy of e³ Σ^- is 28 420 cm⁻¹, which is smaller than the observed data by about 700–750 cm⁻¹. It is noted that the agreement between the observed and calculated ω_e values for the e³ Σ^- state is reasonably good. The calculated r_e of e³ Σ^- is found to be larger than the value estimated from the perturbations in the A¹ Π –X¹ Σ^+ system by interactions with low-lying states including e³ Σ^- .

Three singlets originating from the $... \sigma^2 \sigma^{*2} \sigma'^2 \pi^3 \pi^*$ configuration are denoted as C¹ Σ^- , D¹ Δ , and E¹ Σ^+ . The C¹ Σ^- and D¹ Δ states are more strongly bound than E¹ Σ^+ . Both C¹ Σ^- and D¹ Δ states are represented predominantly by the $\pi \rightarrow \pi^*$ excited configuration with $c^2 \sim 0.86$, while the E¹ Σ^+ state has only 36% contribution of the $... \sigma^2 \sigma^{*2} \sigma'^2 \pi^3 \pi^*$ configuration. A closed-shell configuration $... \pi^4$ ($c^2 = 0.26$) and a doubly excited configuration such as $... \pi^2 \pi^{*2}$ ($c^2 = 0.11$) also contribute strongly in the representation of the E¹ Σ^+ state even at the equilibrium bond length. Of these three singlets, only E¹ Σ^+ undergoes a strong transition to the ground state. There are numerous experimental studies of the E–X band system. Figure 1a shows a very smooth potential energy curve for the E¹ Σ^+ state, which dissociates into the lowest asymptote. The state is found to be comparatively weakly bound. The computed transition energy of this state is 41 383 cm⁻¹ as compared with the observed value of 41 915.8 cm⁻¹. The MRDCI-estimated ω_e of E¹ Σ^+ agrees very well with the observed value of 405.6 cm⁻¹. As seen in Table 2, the small-scale CI calculations of Robbe et al.²⁰ have reported considerably large T_e and small ω_e for the E¹ Σ^+ state. The calculated equilibrium bond length of this state is 2.286 Å (4.32 a_0), which is about 0.027 Å longer than the experimental value reported by Harris et al.¹⁵ The C¹ Σ^- and D¹ Δ states are found to be nearly degenerate, and their potential energy curves look alike (Figure 1a). Spectroscopic constants of C and D states are also very similar in magnitude. Transitions from both C¹ Σ^- and D¹ Δ states to the ground state are not allowed. However, with the inclusion of the spin–orbit coupling, the D¹ Δ_1 –X¹ Σ_0^+ transition would show some intensity.

The b³ Π state of SiS is found to be reasonably strongly bound (binding energy ~ 2.48 eV) with $r_e = 2.026$ Å (3.83 a_0) and $\omega_e = 604$ cm⁻¹. No experimental r_e is available for comparison. We may expect the observed Si–S bond in the b³ Π state to be shorter by 0.03–0.05 Å. The computed transition energy $T_e = 27 378$ cm⁻¹ for the b³ Π state agrees well with the observed values. The spin-forbidden b³ Π –X¹ Σ^+ system has been identified by Linton¹⁴ in the chemiluminescent emission from the reaction of silicon atoms with carbon oxysulfide. Transition

energies of $b^3\Pi_0^+$ and $b^3\Pi_1$ components are reported to be $27\,314.5 \pm 2.2$ and $27\,407.9 \pm 1.1$ cm^{-1} , respectively. The assignment of the observed ultraviolet $b^3\Pi-X^1\Sigma^+$ band has made some doubt because the extrapolated position of the 0–0 band ($^3\Pi$, $\Omega = 1$) reported by Bredohl et al.¹³ is $29\,865$ cm^{-1} . The MRDCI-estimated vibrational frequency of the $b^3\Pi$ state is also in good agreement with the observed data of Linton.¹⁴ The $b^3\Pi$ state arises mainly due to the $\sigma' \rightarrow \pi^*$ excitation. However, two doubly excited configurations such as $... \sigma^2 \sigma'^* \sigma'^2 \pi^3 \pi^{*2}$ ($c^2 = 0.12$) and $... \sigma^2 \sigma'^* \sigma'^2 \pi^3 \pi^{*2}$ ($c^2 = 0.06$) are also important for the description of the $b^3\Pi$ state. It is noted that the σ' MO is strongly bonding combinations of $s(\text{Si})$, $p_x(\text{Si})$, and $p_x(\text{S})$ atomic orbitals. The $\sigma' \rightarrow \pi^*$ transition makes the Si–S bond in the $b^3\Pi$ state weaker than the ground-state bond. Transition probabilities of both $b^3\Pi_1-X^1\Sigma_0^+$ and $b^3\Pi_0^+-X^1\Sigma_0^+$ are also the subject of the present study. The $b^3\Pi-X^1\Sigma^+$ transition may be compared with the spin-forbidden Cameron bands of the isovalent CO.

The same $\sigma' \rightarrow \pi^*$ excitation generates the singlet counterpart of $^3\Pi$. The state is designated as $A^1\Pi$ in accordance with the observed ultraviolet band of the $A^1\Pi-X^1\Sigma^+$ system of SiS. Originally, this band has been assigned by Barrow and co-workers^{5,6} as $D^1\Pi-X^1\Sigma^+$, and later on it has been renamed as the A–X system. The rotational structure of the A–X system shows perturbations of the $A^1\Pi$ state by several other states such as $^3\Sigma^-$, $^1\Sigma^-$, $^3\Delta$, and $^1\Delta$. The computed transition energy of the $A^1\Pi$ state ($T_e = 35\,385$ cm^{-1}) is in excellent agreement with the observed A–X band around $35\,026$ cm^{-1} . The small-scale CI calculations of Robbe et al.²⁰ have overestimated T_e by 3000 cm^{-1} . The A–X transition is expected to be quite strong as observed. The MRDCI-estimated r_e and ω_e of $A^1\Pi$ are 2.112 Å ($3.99 a_0$) and 485 cm^{-1} , respectively. The rotational analysis of the A–X band estimates $r_e = 2.059$ Å for the $A^1\Pi$ state. The ω_e value is underestimated in the present calculations by 28 cm^{-1} . Figure 1a shows a smooth potential energy curve of the $A^1\Pi$ state, which dissociates into the lowest asymptote.

Potential energy curves of the high-lying singlets such as $3^1\Sigma^+$, $4^1\Sigma^+$, $2^1\Sigma^-$, and $2^1\Delta$ are shown in Figure 1a. A broad minimum around $5.30 a_0$ in the potential curve of the $3^1\Sigma^+$ state has appeared due to an avoided crossing. This is confirmed by analyzing compositions of CI wave functions of $E^1\Sigma^+$ and $3^1\Sigma^+$ states at different bond distances. It has been noted that the $E^1\Sigma^+$ state at a longer bond length (say, $r > 6.0 a_0$) is represented mainly by $... \pi^2 \pi^{*2}$, which is the dominant configuration of the $3^1\Sigma^+$ state at a shorter bond length. The compositions of $E^1\Sigma^+$ and $3^1\Sigma^+$, therefore, interchange at longer bond distances of the potential energy curves. The potential curve of the $4^1\Sigma^+$ state has shown an avoided crossing around $4.5 a_0$. At the bond length of 1.973 Å ($3.73 a_0$), there exists a minimum for the $4^1\Sigma^+$ state with $\omega_e = 686$ cm^{-1} and $T_e = 64\,288$ cm^{-1} . This state may have some Rydberg character. The spectroscopic properties of the $4^1\Sigma^+$ state as estimated in the present calculations may not be considered very accurate, as the basis sets do not include Rydberg functions adequately. The potential curves of $2^1\Sigma^-$ and $2^1\Delta$ states are almost repulsive in nature.

Both $^5\Pi$ and $^5\Sigma^+$ states correlating with the lowest asymptote are very weakly bound (binding energy ~ 0.22 eV). The $^5\Pi$ state is represented by a doubly excited configuration such as $... \sigma' \pi^3 \pi^{*2}$ ($c^2 = 0.80$), while the lower-lying $^5\Sigma^+$ state is characterized by another dominant configuration $... \sigma'^2 \pi^2 \pi^{*2}$ ($c^2 = 0.77$). Transition energies of these two quintets are estimated to be around $45\,000$ cm^{-1} . The equilibrium bond length of SiS in the $^5\Pi$ state is calculated to be 2.342 Å ($4.43 a_0$), whereas for the $^5\Sigma^+$ state $r_e = 2.904$ Å ($5.49 a_0$). All other quintet states,

TABLE 3: Dissociation Relation between Ω States and Atomic States of SiS^a

Ω states	atomic states	expt energy/ cm^{-1}
$0^+, 1, 2$	$^3P_0 + ^3P_2$	0
$0^+, 0^-(2), 1(3), 2(2), 3$	$^3P_1 + ^3P_2$	77
$0^+(3), 0^-(2), 1(4), 2(3), 3(2), 4$	$^3P_2 + ^3P_2$	223
$0^-, 1$	$^3P_0 + ^3P_1$	397
$0^+(2), 0^-, 1(2), 2$	$^3P_1 + ^3P_1$	474
0^+	$^3P_0 + ^3P_0$	574
$0^+, 0^-(2), 1(3), 2(2), 3$	$^3P_2 + ^3P_1$	620
$0^-, 1$	$^3P_1 + ^3P_0$	651
$0^+, 1, 2$	$^3P_2 + ^3P_0$	797

^a Reference 41.

TABLE 4: Spectroscopic Constants of Ω States of SiS

state	T_e/cm^{-1}	$r_e/\text{Å}$	ω_e/cm^{-1}
$X^1\Sigma_0^+$	0	1.957	730
$a^3\Sigma_1^+$	23 464	2.198	508
$a^3\Sigma_0^+$	23 482	2.196	504
$d^3\Delta_3$	26 398	2.220	482
$d^3\Delta_2$	26 430	2.221	478
$d^3\Delta_1$	26 553	2.219	485
$b^3\Pi_0^+$	27 180	2.027	590
$b^3\Pi_0^-$	27 205	2.030	594
$b^3\Pi_1$	27 304	2.030	588
$b^3\Pi_2$	27 407	2.027	591
$C^1\Sigma_0^-$	28 195	2.254	460
$e^3\Sigma_1^-$	28 400	2.242	462
$e^3\Sigma_0^-$	28 407	2.244	457
$D^1\Delta_2$	28 563	2.262	446
$A^1\Pi_1$	35 333	2.114	484
$E^1\Sigma_0^+$	41 359	2.284	418
$^5\Pi_3$	44 671	2.335	283
$^5\Pi_2$	44 764	2.341	281
$^5\Pi_1$	44 897	2.342	276
$^5\Pi_0^+$	44 939	2.345	276
$^5\Pi_0^-$	44 949	2.343	276
$^5\Pi_1$	45 075	2.362	257

namely, $^5\Sigma^-$, $2^5\Sigma^+$, $^5\Delta$, and $2^5\Pi$, correlating with the $\text{Si}(^3P_g) + \text{S}(^3P_g)$ limit are repulsive (see Figure 1c). There is an avoided crossing between the curves of $^5\Sigma^-$ and $2^5\Sigma^-$ near $4.5 a_0$. A minimum has appeared in the potential energy curve of the $3^5\Sigma^+$ state around $4.5 a_0$. An avoided crossing in the same curve is also noted around $5.0 a_0$.

Dissociation energies of many silicon compounds have been derived from long extrapolations of the vibrational levels. The ground-state dissociation energy (D_0^0) of $^{28}\text{Si}^{32}\text{S}$ obtained from a short extrapolation of the vibrational levels of the E state assuming its dissociation into $^3P_2 + ^3P_2$ is reported to be 6.42 eV.^{5,8,40} The dissociation energy (D_e) estimated in the present CI calculations is about 5.85 eV, which is an underestimation of the experimentally derived value. It may be noted that similar discrepancies have been noted in all previous calculations using the present methodology. In a recent calculation²¹ on the isovalent GeS molecule, the computed ground-state D_e value is smaller than the observed value by 0.58 – 0.84 eV. The D_e values of the $A^1\Pi$ and $E^1\Sigma^+$ states of SiS estimated from the extrapolation of the vibrational levels have yielded 2.3 and 1.2 eV, respectively.⁵ The MRDCI-estimated dissociation energies of these two states are substantially low (1.45 and 0.72 eV, respectively). Such a discrepancy is probably due to the use of the effective core potential approximation and inadequate basis

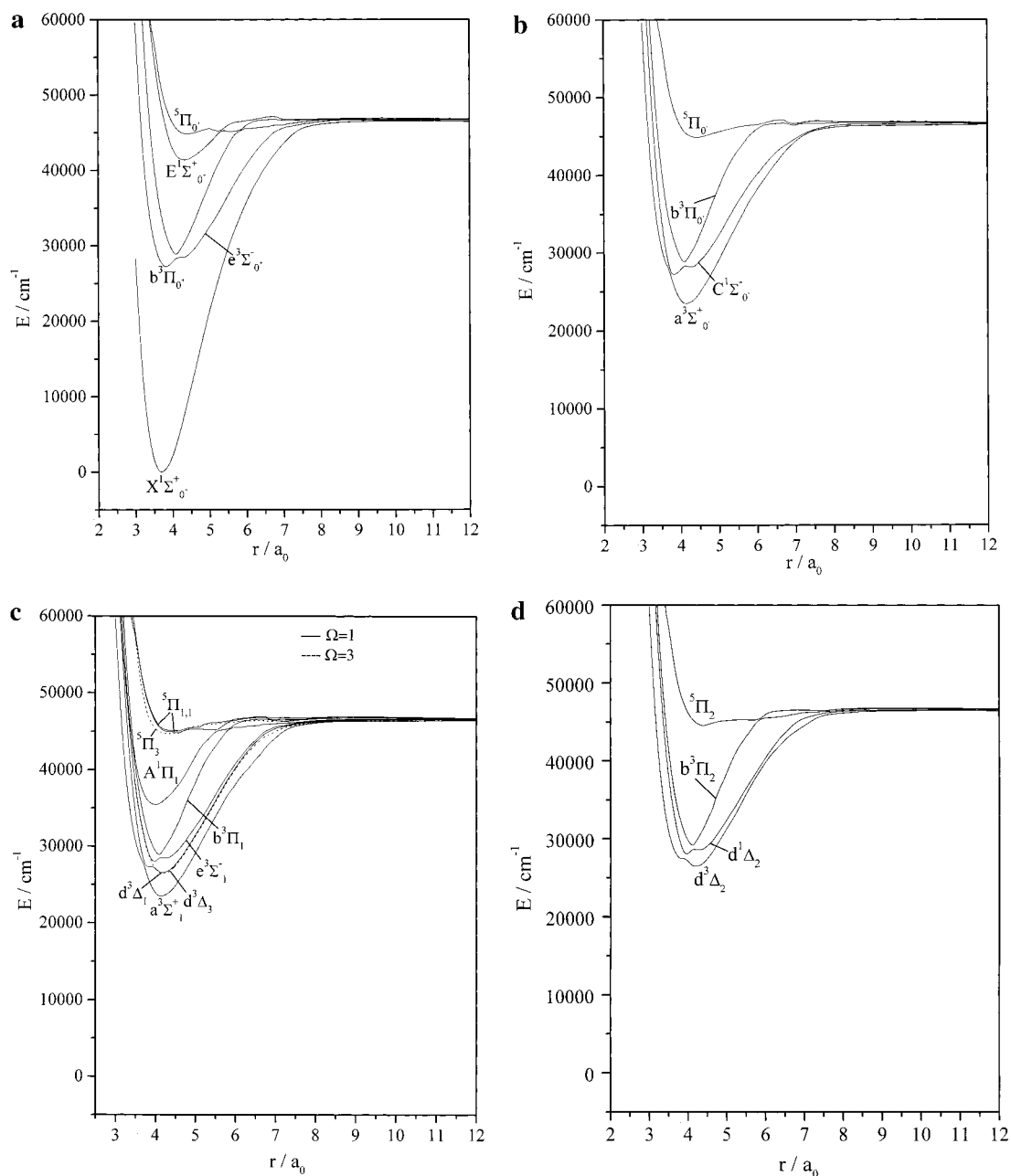


Figure 2. (a) Potential energy curves of low-lying 0^+ states of SiS. (b) Potential energy curves of low-lying 0^- states of SiS. (c) Potential energy curves of low-lying 1 and 3 states of SiS (curves with dashed lines are for $\Omega = 3$). (d) Potential energy curves of low-lying 2 states of SiS.

sets. However, for confirmation, one needs to carry out all electron calculations, which are beyond the scope of the present work.

IV. Spectroscopic Properties and Potential Energy Curves of Ω States

The spin-orbit interaction is introduced in the second step of calculations through the spin-orbit operators for both Si and S as derived from RECP by Pacios and Christiansen.²⁴ All 18 Λ -S states, which correlate with the lowest dissociation limit ($\text{Si}(^3P_g) + \text{S}(^3P_g)$), are allowed to interact through the spin-orbit coupling. Table 3 displays the correlation of Ω states with the atomic states at the dissociation limit along with their observed relative energies. There are 50 Ω states of 0^+ , 0^- , 1, 2, 3, and 4 symmetries, which split into closely spaced nine asymptotes within 800 cm^{-1} only. The computed potential energy curves of some of these Ω states are drawn in Figure

2a–d. The estimated spectroscopic constants of 22 Ω states within $45\,000 \text{ cm}^{-1}$ are displayed in Table 4. The ground-state component ($X^1\Sigma_0^+$) is not perturbed by the spin-orbit coupling. Figure 2a reveals that there are no nearby 0^+ components in the Franck–Condon region for interactions with the ground state. As shown in Table 3, there are 10 $\Omega = 0^+$ states correlating with seven dissociation limits. We have shown only five low-lying curves of 0^+ states in Figure 2a. Other 0^+ curves are mostly repulsive in nature. Two components ($0^-, 1$) of the $a^3\Sigma^+$ state are separated only by 18 cm^{-1} . The present calculations suggest that the $a^3\Sigma_1^+$ component is lower than $a^3\Sigma_0^+$. It may be mentioned here that the $a^3\Sigma_1^+$ component is important from the experimental point of view as the $a^3\Sigma^+ - X^1\Sigma^+$ band has been observed in the region $385\text{--}600 \text{ nm}$ from the chemiluminescent flame spectra of the SiS molecule. The $a^3\Sigma_1^+ - X^1\Sigma_0^+$ transition is supposed to take place with some intensity. Three components of the $d^3\Delta$ state split in the

increasing order of energy ${}^3\Delta_3 < {}^3\Delta_2 < {}^3\Delta_1$. Spectroscopic properties of these components remain almost unchanged. However, the ${}^1\Delta_2$ component interacts with ${}^3\Delta_2$ to a small extent. Four components of the $b^3\Pi$ state split in a regular order, and the largest splitting among the components of this state is computed to be 227 cm^{-1} only. We have fitted the diabatic curves of each component for the estimation of spectroscopic parameters. Experimentally, the $b^3\Pi_r-X^1\Sigma^+$ band has been observed in the chemiluminescent flame spectra. The observed transition energies of $b^3\Pi_{0+}$ and $b^3\Pi_1$ components for their transitions to $X^1\Sigma_{0+}^+$ are $27\,314.5 \pm 2.2$ and $27\,407.9 \pm 1.1\text{ cm}^{-1}$, respectively, in good agreement with the values computed here (see Table 4). Transition properties of both $b^3\Pi_{0+}-X^1\Sigma_{0+}^+$ and $b^3\Pi_1-X^1\Sigma_{0+}^+$ transitions are discussed in the next section.

In general, potential energy curves in Figure 2a-d show several sharp avoided crossings with the curves of nearby components of the same symmetry. The $C^1\Sigma_0^-$ and $D^1\Delta_2$ components are not much perturbed due to the spin-orbit coupling. The spin-orbit splitting between the components of $e^3\Sigma^-$ is calculated to be negligibly small. Both curves of $e^3\Sigma_{0+}^-$ and $e^3\Sigma_1^-$ components undergo avoided crossings near $r = 4.2\text{ a}_0$. Although the spin-orbit coupling is very weak, both the components of $e^3\Sigma^-$ should undergo allowed-transitions to the ground state around $28\,400\text{ cm}^{-1}$. The computed transition energy of the $A^1\Pi_1$ component at the equilibrium bond length is $35\,333\text{ cm}^{-1}$. The $A^1\Pi_1-X^1\Sigma_{0+}^+$ band system has been experimentally studied by several authors, and the transition is expected to be very strong. In the Franck-Condon region of the $A^1\Pi_1$ curve, there is no mixing with any other component of the same symmetry. The potential energy curve and spectroscopic constants of the $E^1\Sigma_{0+}^+$ component do not change significantly due to the spin-orbit interaction (see Figure 2a and Table 4). We have also estimated the spectroscopic properties of six components of ${}^5\Pi$, which has a very shallow potential well. The components split in the inverted energetic order such as 3, 2, 1, 0^+ , 0^- , 1. The largest spin-orbit splitting is found to be only 400 cm^{-1} . None of these components is strongly bound, and transitions from any of these components of ${}^5\Pi$ are, therefore, difficult to observe.

V. Transition Dipole Moments and Radiative Lifetimes

At the Λ -S level, $A^1\Pi$, $E^1\Sigma^+$, $3^1\Sigma^+$, and $4^1\Sigma^+$ states undergo symmetry-allowed transitions to the ground state. Of these, the high-lying $3^1\Sigma^+$ and $4^1\Sigma^+$ states are not considered to be very accurate. Therefore, we have focused on transition dipole moments of $A^1\Pi-X^1\Sigma^+$ and $E^1\Sigma^+-X^1\Sigma^+$ transitions using MRDCI energies and wave functions. Transition probabilities of some other singlet-singlet transitions, such as $A^1\Pi-C^1\Sigma^-$, $A^1\Pi-D^1\Delta$, and $E^1\Sigma^+-A^1\Pi$, and triplet-triplet transitions, such as $b^3\Pi-a^3\Sigma^+$, $e^3\Sigma^- - b^3\Pi$, and $b^3\Pi-d^3\Delta$, are computed in the present study. Transition dipole moments of these transitions as a function of the bond distance are plotted in Figure 3a. It is noted that transition moments of the E-X transition are comparatively much larger in magnitude than those of other transitions. As for example, in the Franck-Condon region, transition-moment values of E-X are at least 4 times larger than those of the A-X transition. The transition-moment curve of the E-X transition shows a maximum in the Franck-Condon region, while for the A-X transition, the curve is monotonically decreasing with the bond length. For other transitions, the calculated transition moments are found to be considerably small. Therefore, $b^3\Pi-a^3\Sigma^+$, $e^3\Sigma^- - b^3\Pi$, and $b^3\Pi-d^3\Delta$ transitions are expected to be weak. The estimated radiative lifetime of the $e^3\Sigma^-$ state at $v' = 0$ is only 0.65 s , while for the $b^3\Pi$

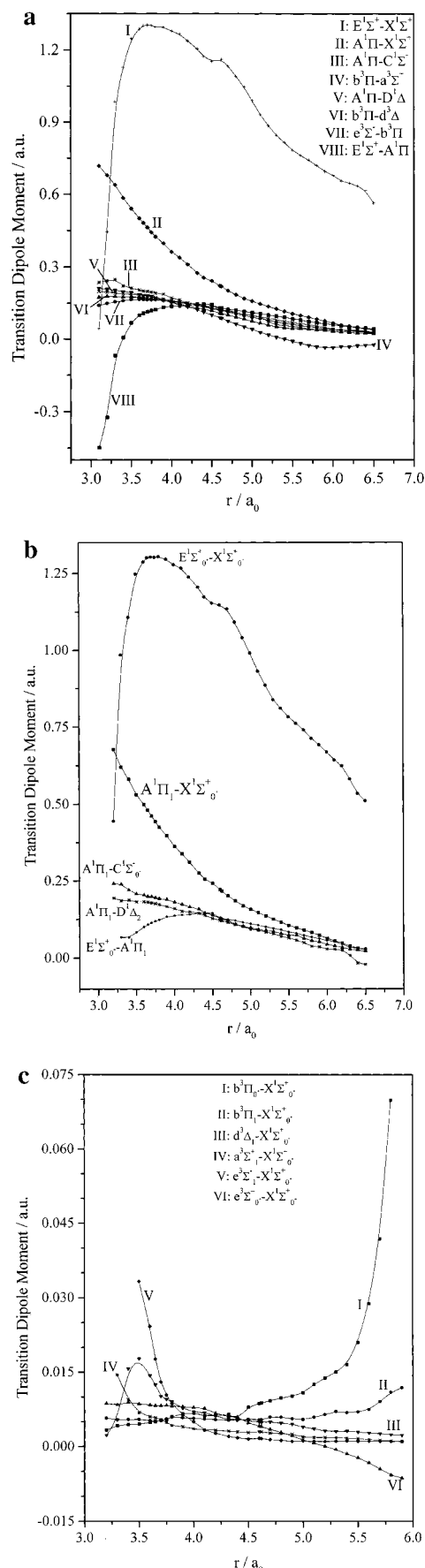


Figure 3. (a) Transition-moment functions of eight transitions involving Λ -S states. (b) Transition-moment functions of five transitions involving spin components of singlet states. (c) Transition-moment functions of spin-forbidden transitions involving spin components of triplets and singlets.

TABLE 5: Radiative Lifetime(s) of Low-Lying Λ -S States of SiS at the Lowest Three Vibrational Levels^a

transition	lifetime of the upper state			total lifetime of the upper state at $v' = 0$
	$v' = 0$	$v' = 1$	$v' = 2$	
$E^1\Sigma^+ - X^1\Sigma^+$	1.01 (-8)	1.25 (-8)	1.32 (-8)	$\tau(E^1\Sigma^+) = 1.01 (-8)$
$A^1\Pi - X^1\Sigma^+$	1.04 (-7)	1.04 (-7)	1.05 (-7)	$\tau(A^1\Pi) = 1.04 (-7)$
$e^3\Sigma^- - b^3\Pi$	6.46 (-1)	5.63 (-2)	1.51 (-2)	$\tau(e^3\Sigma^-) = 6.46 (-1)$
$b^3\Pi - a^3\Sigma^+$	1.45 (-3)	7.60 (-4)	5.39 (-4)	
$b^3\Pi - d^3\Delta$	1.97	6.01 (-2)	1.25 (-2)	$\tau(b^3\Pi) = 1.45 (-3)$

^a Values in parentheses are the powers to base 10.

state, the value is 1.45 ms. The radiative lifetimes of the excited $A^1\Pi$ and $E^1\Sigma^+$ states at the lowest three vibrational levels are shown in Table 5. The E-X transition is found to be at least 10 times stronger than the A-X transition. The $E^1\Sigma^+$ state is found to be short-lived with $\tau = 10.1$ ns at $v' = 0$, while the lifetime of $A^1\Pi$ at the lowest vibrational level is about 100 ns.

As mentioned before, spin-forbidden transitions such as $b^3\Pi - X^1\Sigma^+$ and $a^3\Sigma^+ - X^1\Sigma^+$ have been observed in chemiluminescent flame spectra of the SiS molecule. We have computed transition probabilities of these transitions as well as several other transitions involving the singlet-state components. Figure 3b shows the transition dipole moment curves of some of the transitions involving the spin-orbit components of singlet states, while those of the spin-forbidden transitions involving components of triplet and singlet states are shown in Figure 3c. The $E^1\Sigma_0^+$ component may undergo several transitions to the lower components such as $X^1\Sigma_0^+$, $a^3\Sigma_1^+$, $d^3\Delta_1$, $b^3\Pi_0^+$, $b^3\Pi_1$, $e^3\Sigma_0^-$, $e^3\Sigma_1^-$, and $A^1\Pi_1$. The transition moments of $E^1\Sigma_0^+ - X^1\Sigma_0^+$ are computed to be very large compared with those of other transitions originating from $E^1\Sigma_0^+$. Although, the Franck-Condon overlap factor between the curves of E and X is small due to the shifted equilibrium bond lengths of these two states, the $E^1\Sigma_0^+ - X^1\Sigma_0^+$ transition has been found to be the strongest of all. Transition probabilities of other transitions from $E^1\Sigma_0^+$, especially to those involving triplet-state components are negligibly small. However, the computed transition moments are comparatively large but a small energy gap and Franck-Condon overlap term make the $E^1\Sigma_0^+ - A^1\Pi_1$ transition weak. The estimated total lifetime of $E^1\Sigma_0^+$ at $v' = 0$ is computed to be 10.2 ns. Transitions from $E^1\Sigma_0^+$ through other channels do not change the lifetime of the $E^1\Sigma_0^+$ component significantly. The abrupt rise in the transition moment at longer bond lengths ($r > 5.5 a_0$) in curve I of Figure 3c is because of the increase in the contribution of $E^1\Sigma^+$ in the composition of $b^3\Pi_0^+$.

The partial and total lifetimes of the $A^1\Pi_1$ component involving three transitions are reported in Table 6. The $A^1\Pi_1 - X^1\Sigma_0^+$ transition is reasonably strong, while $A^1\Pi_1 - C^1\Sigma_0^-$ and $A^1\Pi_1 - D^1\Delta_2$ transitions are weak. However, there are other channels for decaying the $A^1\Pi_1$ state through transitions to the lower components such as $a^3\Sigma_{1,0}^-$, $d^3\Delta_{2,1}$, $b^3\Pi_{0^+,0^-,1,2}$, and $e^3\Sigma_{1,0}^-$. Our calculations show that transition dipole moments of all these spin-forbidden transitions are negligibly small. Therefore, these weak transitions do not change the overall lifetime of the $A^1\Pi_1$ component. At the lowest vibrational level, the total lifetime of $A^1\Pi_1$ is estimated to be 10.3 ns. Both the components of $e^3\Sigma^-$ undergo spin-forbidden transitions to the ground-state component. The present calculations predict the $e^3\Sigma_0^- - X^1\Sigma_0^+$ transition to be stronger than $e^3\Sigma_1^- - X^1\Sigma_0^+$. The partial lifetimes of $e^3\Sigma_0^-$ and $e^3\Sigma_1^-$ components are found to be 0.95 and 8.78 ms, respectively. Transition probabilities of the analogous Cameron band, which corresponds to the spin-forbidden transitions such as $b^3\Pi_0^+ - X^1\Sigma_0^+$ and $b^3\Pi_1 - X^1\Sigma_0^+$,

TABLE 6: Radiative Lifetimes(s) of Low-Lying Spin-Orbit States of SiS at the Lowest Three Vibrational Levels^a

transition	lifetime of the upper state			total lifetime at $v' = 0$
	$v' = 0$	$v' = 1$	$v' = 2$	
$E^1\Sigma_0^+ - X^1\Sigma_0^+$	1.02(-8)	1.25(-8)	1.33(-8)	$\tau(E^1\Sigma_0^+) = 1.02(-8)$
$A^1\Pi_1 - X^1\Sigma_0^+$	1.03(-7)	1.03(-7)	1.05(-7)	
$A^1\Pi_1 - C^1\Sigma_0^-$	7.65(-5)	7.28(-5)	6.65(-5)	
$A^1\Pi_1 - D^1\Delta_2$	1.07(-4)	9.96(-4)	9.15(-5)	$\tau(A^1\Pi_1) = 1.03(-7)$
$e^3\Sigma_0^- - X^1\Sigma_0^+$	9.52(-4)	6.94(-4)	8.04(-4)	$\tau(e^3\Sigma_0^-) = 9.52(-4)$
$e^3\Sigma_1^- - X^1\Sigma_0^+$	8.78(-3)	8.33(-3)	4.17(-3)	$\tau(e^3\Sigma_1^-) = 8.78(-3)$
$b^3\Pi_0^+ - X^1\Sigma_0^+$	6.77(-4)	7.73(-4)	9.54(-4)	
$b^3\Pi_0^+ - a^3\Sigma_1^+$	2.63(-3)	1.49(-3)	1.19(-3)	$\tau(b^3\Pi_0^+) = 5.38(-4)$
$b^3\Pi_1 - X^1\Sigma_0^+$	7.08(-4)	9.11(-4)	8.86(-4)	$\tau(b^3\Pi_1) = 7.08(-4)$
$d^3\Delta_1 - X^1\Sigma_0^+$	1.28(-3)	2.35(-3)	1.15(-3)	$\tau(d^3\Delta_1) = 1.28(-3)$
$a^3\Sigma_1^+ - X^1\Sigma_0^+$	7.19(-3)	8.25(-3)	7.34(-3)	$\tau(a^3\Sigma_1^+) = 7.19(-3)$

^a Values in parentheses are the powers to the base 10.

are also calculated in this study. The radiative lifetimes of these bands are in the 500–700 μ s range. There are other weak transitions from the spin components of the $b^3\Pi$ state. The partial lifetime of the $b^3\Pi_0^+ - a^3\Sigma_1^+$ transition is computed to be 2.6 ms. The $d^3\Delta_1$ component undergoes weak spin-forbidden transition to the ground-state component. The radiative lifetime of this component at $v' = 0$ is estimated to be 1.28 ms. The computed transition probability data of the $a^3\Sigma_1^+ - X^1\Sigma_0^+$ transition predict the transition to be fairly weak, and the radiative lifetime of $a^3\Sigma_1^+$ is only 7.19 ms.

VI. Conclusion

Relativistic MRDCI calculations employing effective core potentials have predicted a large number of electronic states of the silicon monosulfide molecule within 45 000 cm^{-1} of energy. The computed spectroscopic properties of the ground state ($X^1\Sigma^+$) and many low-lying excited states agree well with the observed data. The calculated bond length of SiS in the ground state is 0.028 Å longer than the experimental value of 1.929 Å. Transition energies of $a^3\Sigma^+$, $d^3\Delta$, $C^1\Sigma^-$, $e^3\Sigma^-$, and $E^1\Sigma^+$ states are underestimated by about 600–1000 cm^{-1} , while those of $b^3\Pi$, $D^1\Delta$, and $A^1\Pi$ are more agreeable with the observed values. The MRDCI-estimated equilibrium bond lengths of the low-lying states of SiS are more or less consistently longer than the available experimental values by about 0.05 Å. The largest discrepancy in r_e has been noted with the $D^1\Delta$ state. For the experimentally well-known $E^1\Sigma^+$ state, the agreement between the computed and observed spectroscopic constants is reasonably good. In general, the computed vibrational frequencies of all the observed states are in excellent agreement with the experimental values. The ground state is not purely represented by closed-shell configuration ($\dots\pi^4$), but a singly excited configuration ($\dots\pi^3\pi^*$) contributes to a small extent. The overall effects of the spin-orbit coupling are not significantly large, and hence the spectroscopic constants do not change much. Potential energy curves of several Ω states show avoided crossings. The present calculations predict that both $E^1\Sigma^+ - X^1\Sigma^+$ and $A^1\Pi - X^1\Sigma^+$ transitions are reasonably strong. The computed transition probability data show that the former transition is at least 10 times stronger than the latter. The estimated radiative lifetimes of $E^1\Sigma^+$ and $A^1\Pi$ are about 10 and 104 ns, respectively. After the inclusion of the spin-orbit coupling, the $E^1\Sigma_0^+ - X^1\Sigma_0^+$ transition remains the strongest one. The spin-forbidden transitions such as $b^3\Pi_0^+ - X^1\Sigma_0^+$ and $b^3\Pi_1 - X^1\Sigma_0^+$ are found to be similar with the Cameron band of the isovalent CO. These

two transitions are also expected to be strong. The radiative lifetimes of $b^3\Pi_{0+}$ and $b^3\Pi_1$ at $v' = 0$ are 0.677 and 0.708 ms, respectively. Of several other spin-forbidden transitions, $e^3\Sigma_{0+}^- - X^1\Sigma_{0+}^+$, $e^3\Sigma_1^- - X^1\Sigma_{0+}^+$, $d^3\Delta_1 - X^1\Sigma_{0+}^+$, and $a^3\Sigma_1^- - X^1\Sigma_{0+}^+$ should have notable intensities. The lifetimes of the upper components of these systems are in the millisecond order.

Acknowledgment. We are grateful to Prof. Dr. R. J. Buenker, Wuppertal, Germany, for making available his MRDCI codes. S.C. thanks the CSIR, India, for the award of Junior Research Fellowship.

References and Notes

- (1) Barrow, R. F.; Jevons, W. *Proc. R. Soc.* **1938**, 169, 45.
- (2) Barrow, R. F. *Proc. Phys. Soc.* **1939**, 51, 267.
- (3) Barrow, R. F.; Vago, E. E. *Proc. Phys. Soc.* **1944**, 56, 79.
- (4) Vago, E. E.; Barrow, R. F. *Nature, London* **1946**, 157, 77.
- (5) Vago, E. E.; Barrow, R. F. *Proc. Phys. Soc.* **1946**, 58, 538.
- (6) Barrow, R. F. *Proc. Phys. Soc.* **1946**, 58, 606.
- (7) Lagerqvist, A.; Nilheden, G.; Barrow, R. F. *Proc. Phys. Soc.* **1952**, 65, 419.
- (8) Robinson, S. J. Q.; Barrow, R. F. *Proc. Phys. Soc.* **1954**, 67, 95.
- (9) Nilheden, G. *Ark. Fys.* **1956**, 10, 19.
- (10) Barrow, R. F.; Deutsch, J. L.; Lagerqvist, A.; Westerlund, B. *Proc. Phys. Soc.* **1961**, 78, 1307.
- (11) Meyer, B.; Smith, J. J.; Spitzer, K. *J. Chem. Phys.* **1970**, 53, 3616.
- (12) Bredohl, H.; Cornet, R.; Dubois, I.; Wildéria, D. *J. Phys. B: At. Mol. Phys.* **1975**, 8, L259.
- (13) Bredohl, H.; Cornet, R.; Dubois, I. *J. Phys. B: At. Mol. Phys.* **1976**, 9, L207.
- (14) Linton, C. *J. Mol. Spectrosc.* **1980**, 80, 279.
- (15) Harris, S. M.; Gottscho, R. A.; Field, R. W.; Barrow, R. F. *J. Mol. Spectrosc.* **1982**, 91, 35.
- (16) Krishnamurthy, G.; Gopal, S.; Saraswathy, P.; Lakshminarayana, G. *Can. J. Phys.* **1983**, 61, 714.
- (17) Marino, C. P.; Guerin, J. D.; Nixon, E. R. *J. Mol. Spectrosc.* **1974**, 51, 160.
- (18) Balasubramanian, K. *Relativistic Effects in Chemistry Part A. Theory and Techniques*; Wiley-Interscience: New York, 1997.
- (19) Balasubramanian, K. *Relativistic Effects in Chemistry Part B. Applications to Molecules and Clusters*; Wiley-Interscience: New York, 1997.
- (20) Robbe, J. M.; Lefebvre-Brion, H.; Gottscho, R. A. *J. Mol. Spectrosc.* **1981**, 85, 215.
- (21) Dutta, A.; Chattopadhyaya, S.; Das, K. K. *J. Phys. Chem.* **2001**, A105, 3232.
- (22) Manna, B.; Das, K. K. *J. Phys. Chem.* **1998**, A102, 214.
- (23) Dutta, A.; Manna, B.; Das, K. K. *Ind. J. Chem.* **2000**, 39A, 163.
- (24) Pacios, L. F.; Christiansen, P. A. *J. Chem. Phys.* **1985**, 82, 2664.
- (25) Ross, B. O.; Siegbahn, P. E. M. *Theo. Chim. Acta* **1970**, 17, 199.
- (26) Anglada, J.; Bruna, P. J.; Peyerimhoff, S. D.; Buenker, R. J. *J. Phys. B: At. Mol. Phys.* **1983**, 16, 2469.
- (27) Dunning, T. H.; Hay, P. J. In *Modern Theoretical Chemistry; Methods of Electronic Structure*; Schaefer, H. F., III, Ed.; Plenum: New York, 1977; Vol. 3.
- (28) Shih, S. K.; Peyerimhoff, S. D.; Buenker, R. J.; Perić, M. *Chem. Phys. Lett.* **1978**, 55, 206.
- (29) Lingott, R. M.; Liebermann, H. P.; Alekseyev, A. B.; Buenker, R. J. *J. Chem. Phys.* **1999**, 110, 11294.
- (30) Buenker, R. J.; Peyerimhoff, S. D. *Theor. Chim. Acta* **1974**, 35, 33.
- (31) Buenker, R. J.; Peyerimhoff, S. D. *Theor. Chim. Acta* **1975**, 39, 217.
- (32) Buenker, R. J. *Int. J. Quantum Chem.* **1986**, 29, 435.
- (33) Buenker, R. J. In *Proceedings of the Workshop on Quantum Chemistry and Molecular Physics*; Burton, P., Ed.; University Wollongong: Wollongong, Australia, 1980.
- (34) Buenker, R. J. In *Studies in Physical and Theoretical Chemistry*; Carbó, R., Ed.; Elsevier: Amsterdam, The Netherlands, 1981; Vol. 21 (Current Aspects of Quantum Chemistry).
- (35) Buenker, R. J.; Phillips, R. A. *J. Mol. Struct. (THEOCHEM)* **1985**, 123, 291.
- (36) Davidson, E. R. In *The World of Quantum Chemistry*; Daudel, R., Pullman, B., Ed.; Reidel: Dordrecht, The Netherlands, 1974.
- (37) Peyerimhoff, S. D.; Buenker, R. J. *Theor. Chim. Acta* **1972**, 27, 243.
- (38) Buenker, R. J.; Peyerimhoff, S. D.; Perić, M. *Chem. Phys. Lett.* **1976**, 42, 383.
- (39) Perić, M.; Runau, R.; Römelt, J.; Peyerimhoff, S. D. *J. Mol. Spectrosc.* **1979**, 78, 309.
- (40) Huber, K. P.; Herzberg, G. In *Molecular Spectra and Molecular Structure*; Van Nostrand Reinhold: Princeton, NJ, 1979; Vol 4 (Constants of Diatomic Molecules).
- (41) Moore, C. E. *Atomic Energy Levels*; National Bureau of Standards: Washington, DC, 1971; Vol 3.